# Progress Toward Externally Powered X-Band Dielectric-Loaded Accelerating Structures

Chunguang Jing, *Member, IEEE*, Wei Gai, John G. Power, Richard Konecny, Wanming Liu, Steven H. Gold, *Fellow, IEEE*, Allen K. Kinkead, Sami G. Tantawi, Valery Dolgashev, and Alexei Kanareykin

***Abstract*—We summarize recent progress in a program to develop externally powered dielectric-loaded accelerating (DLA) structures that can sustain high accelerating gradients. High--power RF tests of earlier structures showed strong multipactor loading. In addition, arcing at dielectric joints between the uniform DLA structure and matching sections at either end limited the achievable gradient. In this paper, we study the onset of multipactor in a DLA structure. We also study the effect of thin-film TiN coatings applied by atomic layer deposition and the effect of a reduction in the inner diameter of the structure. Test results of these structures show significant decreases in multipactor loading. We also test new structure designs that eliminate separate dielectric matching sections and, thus, the requirement for dielectric joints, including a DLA structure using a coaxial coupler and a clamped DLA structure. The clamped structure demonstrated a significantly improved gradient without breakdown.**

***Index Terms*—Dielectric breakdown, dielectric-loaded accelerator, high-power RF, multipactor.**

## I. Introduction

DIELECTRIC-loaded accelerating (DLA) structures, consisting of a cylindrical dielectric liner inside a conducting metal jacket, are under investigation as an alternative to conventional disk-loaded metal structures for high-gradient RF linear accelerators. A joint program is under way at Argonne National Laboratory and the Naval Research Laboratory (NRL), in collaboration with Euclid TechLabs, LLC, and the SLAC National Accelerator Laboratory, to study X-band DLA structures at high accelerating gradients in order to understand the effects that limit their performance. These studies are being carried out at 11.4 GHz using a high-power external RF drive. Previous papers [1], [2] reported on the study of several different test structures at moderate accelerating gradients (~8 MV/m). Those studies investigated two RF effects that required further investigation, strong multipactor loading of the DLA structures, and RF breakdown of the structures, particularly at joints between separate dielectric sections. One of these papers also developed a simple steady-state model to explain the saturated behavior of the multipactor loading. In this paper, we report the results of experimental studies of several new test structures at high RF drive powers. Some of these studies were designed to investigate the behavior of the multipactor and approaches to reduce the multipactor loading. For example, using the same RF couplers and test configuration that were presented in [2], we have explored structures fabricated from a different dielectric, fused silica (quartz), investigated geometrical factor for the same material, and tested the effect of TiN coatings applied with a state-of-the-art coating technique, atomic layer deposition (ALD). All these efforts led to a significant reduction of the RF power absorption by the multipactor. In addition, other studies focused on the suppression of RF breakdown by eliminating the dielectric joints that were the site of most previous breakdown phenomena. The demonstrated accelerating gradient without RF breakdown has been increased to 15 MV/m in one gap-free DLA structure.

Most of the experiments presented in this paper were performed at the NRL X-band Magnicon Facility with the same basic experimental setup described in [1]. However, one experiment, a test of a large-inner-diameter (ID) quartz-based DLA structure, was carried out at the SLAC National Accelerator Laboratory using a similar experimental configuration but employing a klystron rather than a magnicon as the RF driver. The klystron provided a faster rise time drive pulse with an adjustable pulsewidth. In Section II, we present some features of the multipactor that were observed in that experiment. Detailed results of the methods to reduce the multipactor loading are presented in Section III. In Section IV, we report two gap-free DLA structure designs. Their testing results are presented as well. Some new conceptual designs of high-gradient DLA structures are discussed in Section V. One design, a gap-free DLA structure based on a metallized quartz tube, is currently under investigation. In Section VI, a brief conclusion is drawn.

We note that DLA structures are also under study in another context, in which strong RF fields are generated using high-peak-current electron bunches or bunch trains. In this approach,

Manuscript received September 21, 2009; revised October 29, 2009; accepted October 30, 2009. Date of publication January 15, 2010; date of current version June 9, 2010. This work was supported in part by the U.S. Department of Energy, by the Small Business Innovation Research Program, by the High Energy Physics Division, and by the Office of Naval Research.

C. Jing was with the High Energy Physics Division, Argonne National Laboratory, Argonne, IL 60439 USA. He is now with Euclid TechLabs, LLC, Solon, OH 44139 USA (e-mail: jingchg@hep.anl.gov).

W. Gai, J. G. Power, R. Konecny, and W. Liu are with the High Energy Physics Division, Argonne National Laboratory, Argonne, IL 60439 USA (e-mail: wg@hep.anl.gov; jp@hep.anl.gov; rsk@hep.anl.gov; wmliu@hep.anl.gov).

S. H. Gold is with the Plasma Physics Division, Naval Research Laboratory, Washington, DC 20375 USA (e-mail: steven.gold@nrl.navy.mil).

A. K. Kinkead is with Icarus Research, Inc., Bethesda, MD 20824-0780 USA (e-mail: allen.kinkead@nrl.navy.mil).

S. G. Tantawi and V. Dolgashev are with the SLAC National Accelerator Laboratory, Menlo Park, CA 94025 USA (e-mail: tantawi@slac.stanford.edu; dolgash@slac.stanford.edu).

A. Kanareykin is with Euclid TechLabs, LLC, Solon, OH 44139 USA (e-mail: alexkan@euclidtechlabs.com).

Color versions of one or more of the figures in this paper are available online at http://ieeexplore.ieee.org.

Digital Object Identifier 10.1109/TPS.2009.2036921

0093-3813/$26.00 © 2010 IEEE

a very strong wakefield is excited with duration usually in the range of a few nanoseconds. Gradients of 5.5 GV/m on axis at terahertz frequencies and 100 MV/m in the microwave range have been demonstrated [3], [4]. These experiments typically do not observe multipactor loading because the short duration of the RF fields is much less than the multipactor rise time. One goal of the present study is to improve the understanding of multipactor rise times, which may also affect wakefield-driven structures as the RF pulses are lengthened.

## II. Some Observed Characteristics of Multipactor in a DLA Structure

Anomalous RF power loss due to severe multipactor in an externally driven DLA structure was reported in [1], but in fact, this phenomenon was first discovered more than 50 years ago [5]. However, in that case, dielectric washers were used rather than a continuous dielectric liner to construct the DLA structure, and the multipactor was associated with oil contamination of the dielectric surface. In this paper, the phenomenon that we are dealing with is a single-surface multipactor on a clean dielectric liner, in which the trajectories of secondary electrons impact on the same surface from which they were born. However, in the DLA case, there is a strong component of the RF electric field that is normal to the dielectric surface. This is unlike the case of single-surface multipactor on an RF window, where the RF electric fields are tangential. This regime of multipactor was described and analyzed in [1]. At some threshold value of the RF field, seed electrons will impact the surface at sufficient energy to generate secondary electrons with a secondary-electron emission coefficient that exceeds unity, resulting in a secondary-electron avalanche. The saturation process for this avalanche relates to the effect of the space-charge electric fields that are created by the buildup of the secondary-electron cloud since, in the cylindrical geometry of a DLA structure, the secondary-electron space-charge cloud produces an electric field that accelerates the secondary electrons radially outward and back toward the dielectric surface. A large-enough radial space-charge electric field, compared to the RF electric field component that creates the multipactor, leads to saturation of the multipactor process and, thus, to a steady-state loading of the RF transmission through the DLA structure. In steady state, the RF power is absorbed by the secondary electrons and lost through collisions of the electrons with the walls of the structure.

In the winter of 2006, a high-power RF test of a quartz-based DLA structure was carried out at the SLAC accelerating structures testing area facility. In order to focus on the multipactor study and avoid the dielectric joint breakdown that happened in some previous experiments [2], this particular DLA structure was designed to use a low dielectric constant material (3.78 for the fused quartz) and a large beam hole (17.94-mm ID) so that a single section of the quartz tube with slightly tapered ends could achieve a broadband impedance match. However, some of the desirable properties of an accelerating structure were sacrificed: This structure had a low shunt impedance of 27.9 $\mathrm{M}\Omega/\mathrm{m}$, an $R/Q$ of only 3.6 $\mathrm{k}\Omega/\mathrm{m}$, and a low group velocity of 38% of the speed of light.

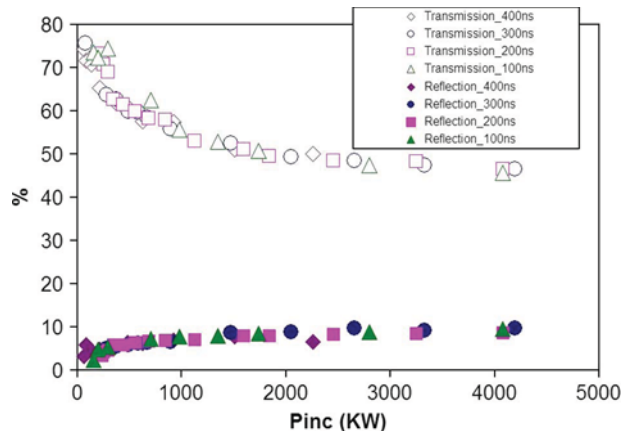


Fig. 1. RF multipactor characteristics of the DLA structure with varying RF pulselength.

In this experiment, we systematically studied the characteristics of the multipactor as a function of the RF pulselength. Fig. 1 shows the behavior of the RF transmission and reflection with pulselength as the pulselength is varied from 100 to 400 ns in 100-ns steps. Unlike the test of an alumina-based DLA structure [1], where the transmission fractions constantly decreased as the incident RF power was increased, the transmission fractions of the quartz structure for all pulselengths leveled off at an $\sim$25% decrease above $\sim$3-MW drive power. A similar saturated behavior was observed in the test of the TiN-coated alumina DLA structure [2]. This, in general, agrees with the characteristics of second electron emission (SEE) yield for quartz and alumina: Quartz has a weaker SEE behavior compared to alumina [6]. The data show that the RF loss from the multipactor is independent of the RF pulselength whenever the pulselength is long enough for the multipactor loading to reach saturation. In addition, another set of measurements studied the relation between the multipactor saturation time and the incident RF power. The saturation time is determined by the buildup time of the secondary-electron cloud to the point that the space-charge field from the secondary electrons becomes large enough to suppress further electron multiplication [1]. As a practical matter, the saturation time of multipactor was measured by the time from the beginning of the RF pulse to the peak of a photomultiplier tube (PMT) signal that was used to monitor the light generated by the multipactor. The data in Fig. 2 show that the multipactor buildup time decreased rapidly when the incident RF power was increased, finally leveling off at $\sim$20 ns. We should point out that readings of the saturation time above 1.5 MW of input power are limited by the PMT rise time ($\sim$5 ns) and response delay ($\sim$3 ns). This suggests that the minimum time to saturation is of order 10 ns. However, it is difficult to determine the minimum time accurately since the rise time of the microwave pulse was also of order 10 ns. Further investigation is needed to characterize this value more accurately. The minimum buildup time of multipactor will depend on the characteristics of the material, as well as the geometry. Note that, for short-enough RF pulses, it is expected that the multipactor will not have time to build up even at very high drive powers.

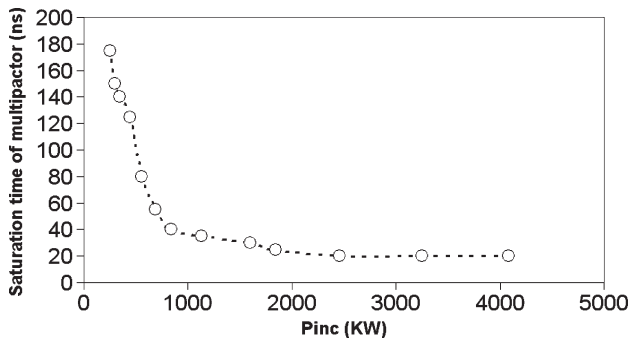


Fig. 2. Dependence of the saturation time of multipactor as a function of the incident RF power. An RF pulsewidth of 200 ns was used.

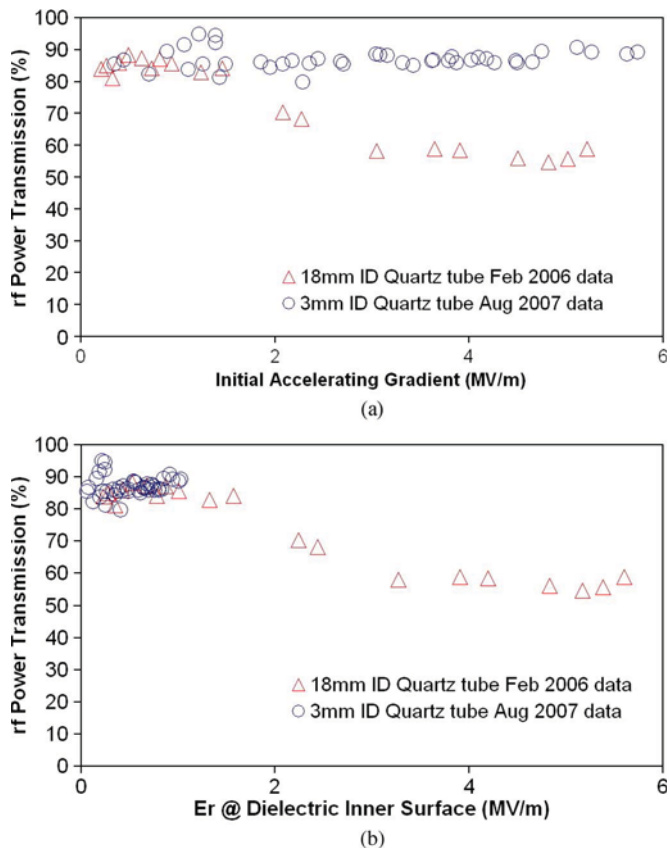


Fig. 3. Comparison of the high-power RF transmission in terms of (a) $E_z$ and (b) $E_r$ in two quartz-based DLA structures with different size beam tunnels.

## III. Techniques to Reduce the Multipactor in DLA Structures

In the past two years, one of our goals has been to investigate approaches to multipactor reduction. We have tested DLA structures using different dielectric materials, different geometries, and with and without low-secondary-emission-coefficient surface coatings. These various experiments were performed at the NRL Magnicon Facility, which can provide up to 20-MW 200-ns (FWHM) RF pulse at 11.43 GHz.

Fig. 3 shows the test results for two quartz-based DLA structures. The two structures were fabricated using the same GE214 fused quartz tube but employed different geometries (different diameters of the beam channel). Based on a physical model for multipactor saturation in a circular DLA structure, the absorbed power due to the multipactor should be proportional to $a^4$ for a certain accelerating gradient, where $a$ is the inner radius of the dielectric tube [7]. This predicted fourth-power dependence is partially due to the $E_r/E_z$ ratio (representing the radial and longitudinal electric field, respectively) of the accelerating mode $(\mathrm{TM}_{01})$ in the DLA structure, which is decreased for smaller ID dielectric tubes. The physical model shows that $E_r$ is the dominant factor that affects the multipactor. Fig. 3(a) shows that the smaller diameter structure showed no evidence of the strong multipactor loading seen in the larger diameter structure. However, when the RF transmission data are replotted versus $E_r$ [shown in Fig. 3(b)], we can see that, in fact, the highest tested $E_r$ value of the smaller ID structure has not yet reached the strong multipactor region seen in the larger ID structure. To some extent, we may say that the multipactor as a function of accelerating gradient can be lowered by reducing the ID of the dielectric tube of the DLA structure. The test of the 3-mm-ID quartz-based DLA structure was ended by RF breakdown at a small crack at one end of the quartz tube.

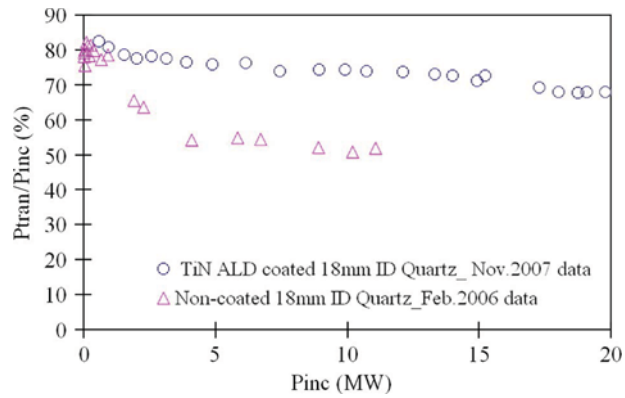


Fig. 4. Comparison of the high-power RF transmission in two quartz-based DLA structures: The TiN surface coated and the noncoated ones.

The use of a TiN coating has previously been demonstrated to reduce the multipactor loading in an alumina-based DLA structure [2]. The coating technique employed was physical vapor deposition (PVD). To further suppress the multipactor, we tried TiN coating on the dielectric surface using ALD, which offers improved coating uniformity. Two sets of dielectric tubes, quartz and alumina, were tested both before and after the coating was applied. In both cases, the thickness of the TiN coating was 1.3 nm. The first TiN ALD-coated structure to be tested was an 18-mm-ID quartz-based DLA structure, which is the same structure discussed in Section II. This structure was tested at high power at the NRL Magnicon Facility under the same set of conditions, both before and after the coating was applied. Fig. 4 shows a comparison of the RF transmission through the structure as a function of incident RF power for both cases. The coated structure showed 20% less RF power loss. Moreover, the same type of 1-cm ID alumina tube that was employed in the experiments described in [2] was coated with a TiN layer using the ALD technique. However, the alumina tube for this experiment was only half the length of the tubes employed in the earlier experiments. Fig. 5 shows a comparison

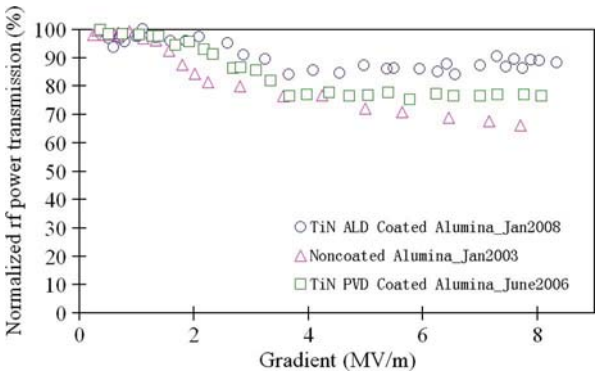


Fig. 5. Comparison of the high-power RF transmission in three alumina-based DLA structures: The TiN ALD surface coated, the TiN PVD surface coated, and the noncoated ones. The RF power transmission is normalized to the value at low gradient prior to the occurrence of multipactor loading.

of the RF transmission through this structure as a function of accelerating gradient compared to the previous results for an uncoated tube and a tube coated with TiN applied by PVD. The losses through the uncoated and PVD-coated structures have been normalized to account for the different structure length, with the assumption that the multipactor power loss is evenly distributed along the length of the dielectric structure. The ALD-coated structure shows a consistent reduction in power loss compared to both of the other structures. The improvement over the PVD-coated structure is perhaps due to the thinner coating, as well as the more accurate control of the coating thickness that ALD provides. It is known that the thickness of the TiN coating plays an important role in reducing the multipactor loading in high-power RF windows because the energy distribution of the second electron yield varies with the coating thickness [8], [9]. The thickness of the TiN coating on the alumina tubes tested in these experiments was 1.3 nm in the ALD-coated case and 20 nm for the coating applied using PVD. (The latter value was provided by the coating firm.) However, the physics underlying multipactor loading of a circular DLA structure is still not fully understood. A complete physical model of the multipactor in this geometry is under investigation [10]. Both the quartz and alumina experiments confirm that a TiN coating can substantially reduce the multipactor loading but not completely eliminate it.

## IV. High-Gradient Gap-Free DLA Structures

In addition to multipactor, another serious issue that can limit the practical application of DLA structures is the occurrence of RF breakdown. Most of the incidents of RF breakdown in the DLA structures studied in this program have occurred at the joints between separate dielectric sections. These breakdowns were attributed to the local field enhancements in the microscale gaps that were present, where the separate dielectric inserts were in physical contact. (Some breakdowns also occurred elsewhere at defects in the dielectric material, such as small chips or cracks.) Such joints were present in all the structures using alumina or magnesium calcium titanate (MCT) inserts but not in the large-ID quartz structures.

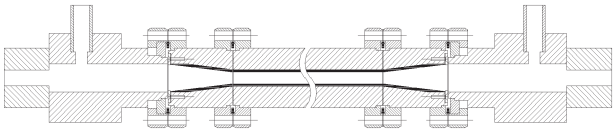

Fig. 6. Schematic drawing of the modular DLA structure which consists of (from left to right) an all-metal TE–TM input coupler, an input tapered dielectric matching section, a constant-radius dielectric accelerating section, an output tapered dielectric matching section, and an all-metal TM–TE output coupler.

In general, the use of a higher dielectric constant material with a smaller ID is always preferred to obtain a higher accelerating gradient (although a larger ID is more favorable for beam transport and to minimize transverse wakefields). In most cases, the cutoff frequency of an empty circular waveguide that houses the dielectric tube is far above the operating frequency of the DLA structure. For high-gradient structures, the circular opening of an X-band $TE_{10}$-mode–$TM_{01}$-mode converter will always be larger than the outer diameter (OD) of the dielectric insert. Therefore, a dielectric-loaded waveguide section with a tapered OD is required for impedance and geometrical matching. Fig. 6 shows the typical configuration of the modular DLA structures that have been employed in these experiments. One advantage of this design is that the broadband TE-mode–TM-mode converter can be reused to test DLA structures with different materials or geometries. However, a single-section dielectric insert whose OD tapers outward at both ends cannot be inserted into a metal tube without leaving a large gap around the central section of the insert. As a result, separate matching sections have been required to ensure that the OD of the dielectric was always in physical contact with the inner surface of the metal tube.

In order to eliminate dielectric joints, two new types of structures were developed that employ a single-section dielectric insert. One uses a coaxial RF coupler, and the other structure uses a clamped metal outer jacket to enclose a tapered dielectric insert.

Fig. 7 shows the gap-free DLA structure based on a coaxial coupler. The coaxial-type coupler implements the $TE_{10}$- to $TM_{01}$-mode conversion through a transient TEM mode so that the mode and impedance transitions can be achieved simultaneously without using a separate tapered dielectric section. In this way, only a straight dielectric tube is needed. At present, ~20-cm-long high-quality low-loss dielectric materials are available [11], limiting the length of our gap-free test structures, but longer sections could be fabricated using a ceramic brazing technique [12]. The coaxial coupler also employs a double-input design to symmetrize the coupling regions in order to eliminate parasitic dipole modes and to minimize beam perturbations that could lead to beam breakup effects in an accelerator. A structure using this scheme was built and has been tested at high power [13]. However, arcing occurred within the input coupler at an input power of a few megawatts during the initial test. Examination after the test showed some chemical residue from the final cleaning process that led to the arcing.

The most recent DLA structure that has been tested is the clamped structure shown in Fig. 8. Instead of using the

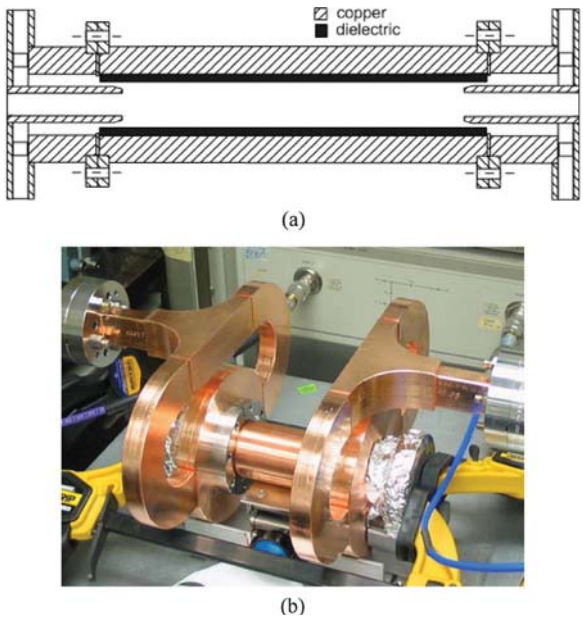


Fig. 7. (a) Two-dimensional view of the coaxial-RF-coupler-based gap-free DLA structure. (b) Coaxial-RF-coupler-based gap-free DLA structure under bench test.

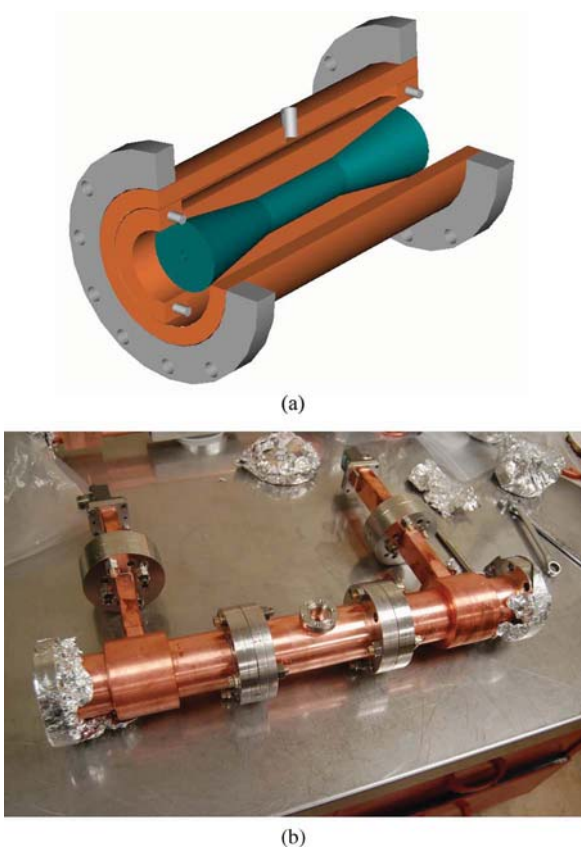


Fig. 8. (a) Three-dimensional view of the clamped DLA structure. (b) Assembled clamped DLA structure using the $TE_{10}-TM_{01}$ high-power RF couplers.

combination of two complicated coaxial RF couplers and a simple dielectric-lined waveguide, we used another gap-free DLA scheme that consists of two well-tested $TE_{10}$-mode–$TM_{01}$-mode converters and a relatively complicated clamped dielectric-loaded waveguide as the central accelerating section. The dielectric tube in this design is fabricated from a single piece of material with both ends flared for impedance matching. The metal boundary at the outside of the dielectric section is provided by a clamped assembly, in which two metal halves enclose the dielectric tube. That, in turn, is placed within an outer metal vacuum jacket. The longitudinal gap along the copper jackets has no effect on the $TM_{01}$ mode (the acceleration mode) since it does not require transverse surface current; instead, only unwanted hybrid modes which have azimuthal surface currents would be disturbed. The outermost copper tube is the vacuum jacket, with an extra pumping port attached at the center.

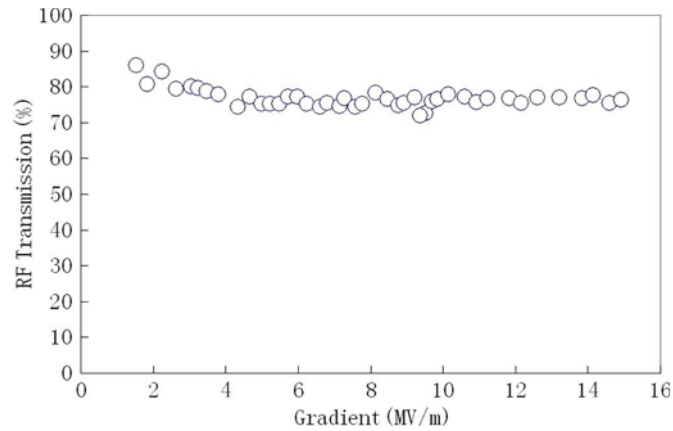


Fig. 9. High-power RF testing results for the quartz-based clamped DLA structure.

We have built one X-band clamped DLA structure using quartz as the loaded material. The ID is 3 mm. This structure is designed to produce an 11.6-MV/m accelerating gradient at 10-MW RF drive. This structure was tested to an input power level of 16.5 MW with no sign of RF breakdown, which results in a gradient of 15 MV/m. The experimental results are plotted in Fig. 9. The 10% RF transmission drop as the power was increased up to 4 MW reflects the onset of the multipactor-induced loss, which also correlated with the fluorescent light that we observed in the experiment. At higher drive power, the RF transmission percentage is flat. This structure showed no sign of RF breakdown at the highest tested powers. We plan to test the structure at still higher drive powers in the future in order to demonstrate higher gradients.

## V. Future Plans

In order to obtain a higher acceleration gradient for a given RF input power and a given ID, a higher permittivity material is required. For example, compared to the quartz-based clamped DLA structure in Section IV, a structure fabricated from MCT-20 ($Mg_xCa_{1-x}TiO_3$, dielectric constant of 20) with the same 3-mm-diameter beam tunnel will produce a 26.4-MV/m gradient at 10-MW incident power. However, the design of the clamped DLA structure described in Section IV may not be suitable for use with this high-permittivity material because the

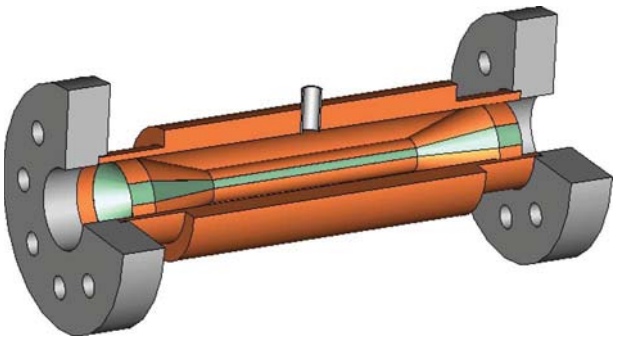

Fig. 10. Design of a gap-free DLA structure using a metallized dielectric tube.

Fig. 11. Metallized dielectric sample tubes using copper sputtering deposition.

surface contact between the outer surface of the dielectric and the clamping metal structure may create a region that cannot be vacuum pumped effectively due to surface nonuniformities caused by machining imperfections. This might result in an RF discharge in this region.

In order to overcome this problem, we are developing a new gap-free structure using a dielectric tube whose outer surface is metallized. Fig. 10 shows the configuration. Basically, the metallization layer of the dielectric tube replaces the copper shell in the previous clamped DLA structure design so that the vacuum gap between the copper and the dielectric surface can be eliminated. The concept of using a metallized dielectric tube is straightforward and has obvious advantages over our previous designs. However, the technology to make a copper coating on the dielectric surface that can meet our requirements (including thickness, bonding strength, and surface roughness) is technically challenging. We have explored various coating techniques, including PVD, ALD, sputtering deposition, metal splashing, etc. Ultimately, we decided to use copper sputtering deposition because it can produce a thick coating ($> 100\ \mu$m) with relatively good bonding to various dielectric materials and can produce a relatively good surface finish.

We are currently evaluating the performance of copper sputtering deposition on quartz, alumina, and cordierite tubes. Fig. 11 shows some sample tubes that have been finished by Southwest Research Institute in Texas. SEM analyses have been performed at Argonne National Laboratory to evaluate some basic parameters of the copper coating, such as the coating

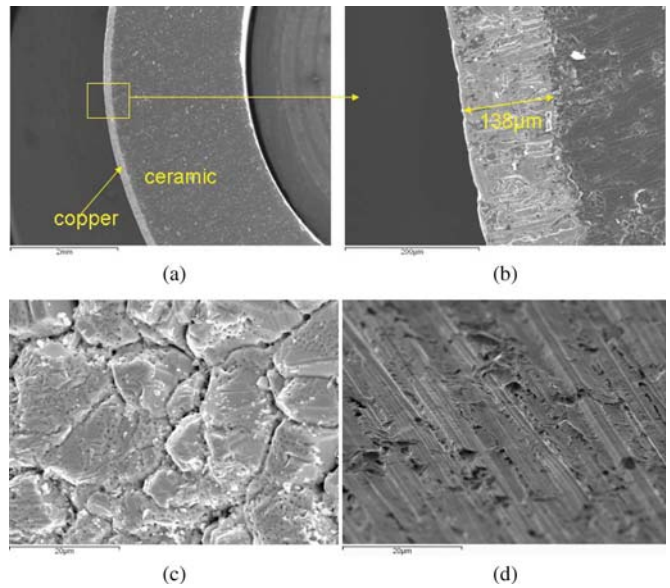


Fig. 12. SEM pictures of the metallized dielectric sample tubes: (a) Edge at 2-mm scale; (b) edge at 200-$\mu$m scale; (c) copper coating surface at 20-$\mu$m scale; (d) surface of the OFE copper at 20-$\mu$m scale after being polished by a fine sandpaper. The ceramic material in the picture is cordierite.

thickness, bonding, and surface finish. In Fig. 12(b), we can see that the $\sim$140-$\mu$m copper layer is uniformly attached to the ceramic surface. The bonding between the two materials also appears to be very strong. However, from Fig. 12(c), we can see that the surface finish is not very smooth. Grain boundaries on the copper surface are very deep. The average surface roughness is measured to be $\sim 2.5\ \mu$m. Particularly in a high-power RF environment (high surface current and/or high electric field), these deep grain boundaries may trigger RF breakdown. As a comparison, Fig. 12(d) shows the surface finish of a regular solid oxygen-free electronic (OFE) copper surface after sandpaper polishing (1000 grit), which is the normal inner surface finish for the copper housing of our previous DLA structures. However, the roughness of the coated surface may not be a problem. One distinct advantage of the DLA structure is that the axial accelerating electric field is the maximum field in the structure and much larger than the fields between the dielectric insert and the metal wall. Thus far, we have never observed RF breakdown on the copper surface of the DLA structures. We are planning to do the final evaluation of the copper sputtering technique in a high-power RF test of a DLA structure constructed in this manner.

## VI. Conclusion

We have made significant progress in the development of externally powered DLA structures. Several new structures have been built and tested at high power to investigate both multipactor and RF breakdown issues. Higher accelerating gradients have been achieved, and we have found that multipactor loading can significantly be reduced through the use of the ALD coating technique. We plan to carry out further studies to understand the limits and the potential of these externally driven DLA structures.

## REFERENCES


[1] J. G. Power, W. Gai, S. H. Gold, A. K. Kinkead, R. Konecny, C. Jing, W. Liu, and Z. Yusof, "Observation of multipactor in an alumina-based dielectric-loaded accelerating structure," *Phys. Rev. Lett.*, vol. 92, no. 16, p. 164 801, Apr. 2004.

[2] C. Jing, W. Gai, J. G. Power, R. Konecny, S. H. Gold, W. Liu, and A. K. Kinkead, "High-power RF tests on X-band external powered dielectric-loaded accelerating structures," *IEEE. Trans. Plasma Sci.*, vol. 33, no. 4, pp. 1155–1160, Aug. 2005.

[3] M. C. Thompson, H. Badakov, A. M. Cook, J. B. Rosenzweig, R. Tikhoplav, G. Travish, I. Blumenfeld, M. J. Hogan, R. Ischebeck, N. Kirby, R. Siemann, D. Walz, P. Muggli, A. Scott, and R. B. Yoder, "Breakdown limits on gigavolt per-meter electron beam-driven wakefields in dielectric structures," *Phys. Rev. Lett.*, vol. 100, no. 21, p. 214 801, May 2008.

[4] M. E. Conde, "Survey of advanced dielectric wakefield accelerators," in *Proc. Particle Accel. Conf.*, Albuquerque, NM, Jun. 2007, pp. 1899–1903.

[5] R. B. R. Shersby-Harvie, L. B. Mullett, W. Walkinshaw, J. S. Bell, and B. G. Loach, "A theoretical and experimental investigation of anisotropic dielectric-loaded linear electron accelerators," in *Proc. Inst. Elect. Eng.—B*, Jul. 1956, vol. 104, pp. 273–292.

[6] R. A. Kishek and Y. Y. Lau, "Multipactor discharge on a dielectric," *Phys. Rev. Lett.*, vol. 80, no. 1, pp. 193–196, 1998.

[7] J. Power and S. H. Gold, "Multipactor modeling in cylindrical dielectric loaded accelerators," in *Proc. 12th Adv. Accel. Concepts Workshop*, vol. 877, *AIP Conference Proceedings*, M. Conde and C. Eyberger, Eds., Dec. 2006, pp. 362–369.

[8] S. Michizono, A. Kinbara, Y. Saito, S. Yamaguchi, and N. Matuda, "TiN film coatings on alumina radio frequency windows," *J. Vac. Sci. Technol. A, Vac. Surf. Films*, vol. 10, no. 4, pp. 1180–1184, Jul. 1992.

[9] Suharyanto, S. Michizono, Y. Saito, S. Yamano, and S. Kobayashi, "Secondary electron emission of TiN-coated alumina ceramics," *Vacuum*, vol. 81, no. 6, pp. 799–802, Feb. 2007.

[10] O. V. Sinitsyn, G. S. Nusinovich, and T. M. Antonsen, Jr., "Self-consistent nonstationary two-dimensional model of multipactor in dielectric-loaded accelerator structures," *Phys. Plasmas*, vol. 16, no. 7, p. 073 102, Jul. 2009.

[11] [Online]. Available: www.euclidtechlabs.com

[12] R. W. Bruce, R. L. Bruce, A. W. Fliflet, M. Kahn, S. H. Gold, A. K. Kinkead, D. Lewis, III, and M. A. Imam, "Joining of ceramic tubes using a high-power 83-GHz millimeter-wave beam," *IEEE. Trans. Plasma Sci.*, vol. 33, no. 2, pp. 668–678, Apr. 2005.

[13] C. Jing, A. Kanareykin, R. Konecny, J. G. Power, S. H. Gold, and S. Kazakov, "Progress towards a gap-free dielectric-loaded accelerator," in *Proc. Particle Accelerator Conf.*, Albuquerque, NM, Jun. 2007, pp. 3151–3153.


**Chunguang Jing** (M'XX) received the Ph.D. degree in electrical engineering from Illinois Institute of Technology, Chicago, in 2005.

In 2001–2005, as a Graduate Appointee, he was with the High Energy Physics Division, Argonne National Laboratory, Argonne, IL, where he worked on the Argonne Wakefield Accelerator project. Since 2005, he has been a Senior Researcher with Euclid TechLabs, LLC, Solon, OH. His research interests include dielectric-loaded accelerating structures, dielectric-based wakefield RF power extraction, wakefield acceleration, RF and microwave circuits and EM simulation, etc.

**Wei Gai**, photograph and biography not available at the time of publication.

**John G. Power**, photograph and biography not available at the time of publication.

**Richard Konecny**, photograph and biography not available at the time of publication.

**Wanming Liu**, photograph and biography not available at the time of publication.

**Steven H. Gold** (M'86–SM'88–F'96) received the Ph.D. degree in physics from the University of Maryland, College Park, in 1978.

He is currently the Senior Scientist for Radiation Generation Physics with the Beam Physics Branch, Naval Research Laboratory, Washington, DC. His research interests include high-power microwave generation, fast-wave microwave devices, and applications of high-power microwave sources to accelerators and industrial processes. He currently directs a program to study accelerator-related microwave technologies, including active microwave pulse compressors and dielectric-loaded accelerators, using a high-power 11.4-GHz magnicon amplifier tube that he developed. He has published more than 60 journal articles and 100 proceeding papers and is the holder of five U.S. patents and two statutory invention registrations.

Dr. Gold has been actively involved with the IEEE, its Nuclear and Plasma Sciences Society (NPSS), and the NPSS Plasma Science and Applications Committee (PSAC). He has served on the PSAC Executive Committee for 20 years, including three three-year terms as an elected member, two years as Vice Chair, and 11 years as Secretary. He was also an Associate Editor of the IEEE TRANSACTIONS ON PLASMA SCIENCE for 20 years, with special responsibility for the biennial issue on *High Power Microwave Generation*. He has served on the Program Committee of the IEEE International Conference on Plasma Science on a number of occasions and as Session Organizer and Session Chair of many conferences and workshops. He has also served on the NPSS Administrative Committee (AdCom) for more than five years. He is currently a member of the IEEE National Fellow Committee, an elected member of the NPSS AdCom, the Chair of the AdCom Chapters and Local Activities Committee, an NPSS Distinguished Lecturer Coordinator, and the Secretary of PSAC. He is a fellow of the American Physical Society and was the recipient of the 2008 NPSS Richard F. Shea Distinguished Member Award "for outstanding contributions to the IEEE Nuclear and Plasma Sciences Society and its Plasma Science and Applications Technical Committee."

**Allen K. Kinkead** was born in Bristol, TN, on May 31, 1935. He received the B.S. degree from the School of Mechanical Engineering, East Tennessee State University, Johnson City, TN, in 1962 and the M.S. degree in electrical engineering and electronics from The George Washington University, Washington, DC.

From 1962 to 1965, he was with the Apollo Spacecraft Division, North American Aviation Company, where he was involved in the engineering support effort for the Apollo Program. From 1966 to 1990, he was with the Naval Research Laboratory (NRL), where he helped build and operate large electron beam pulse generators, including Gamble I, Gamble II, Triton, and VEBA, worked on projects to develop millimeter-wave gyrotrons, cyclotron autoresonance masers, and free-electron lasers, and managed a facility for microwave vulnerability/susceptibility testing. Following his retirement from NRL in 1990, he was a Consultant by a variety of companies, including Mission Research Corporation and Sachs/Freeman Associates. In 1994, he returned to NRL as a full-time contract employee, where, since then, he became the Chief Engineer responsible for the design, engineering, fabrication, and operations for the NRL magnicon program. He is currently an Onsite Contractor with Icarus Research, Inc., Bethesda, MD. He is the coauthor of more than 25 refereed journal articles, 40 proceeding papers, and 100 scientific conference presentations and is the holder of one patent.

**Sami G. Tantawi**, photograph and biography not available at the time of publication.

**Valery Dolgashev**, photograph and biography not available at the time of publication.

**Alexei Kanareykin**, photograph and biography not available at the time of publication.